

Paper B

**Numerical Investigation of the
Range of Validity of a
Low-Frequency Approximation
for CSEM ***

B

* Published in 72nd EAGE Conference and Exhibition, Barcelona, Expanded Abstracts, P.D34–D38, 2010.

D034

Numerical Investigation of the Range of Validity of a Low-frequency Approximation for CSEM

S. Bakr* (CIPR) & T. Mannseth (CIPR)

SUMMARY

Recently, a novel approximate hybrid method for modeling marine CSEM, simplified integral equation (SIE) modeling, has shown excellent accuracy in modeling the low-frequency response from a thin resistive target in a 2D setting (Bakr and Mannseth, *Geophysics* 74 (5), 2009). SIE solves the Poisson equation in a region containing the target, and subsequently uses rigorous integral equation (IE) modeling to obtain the EM fields in the receivers. SIE thus replaces the computationally intensive dense-matrix part of the rigorous IE method by sparse-matrix calculations based on a low-frequency approximation of Maxwell's equations. The computational performance of SIE was found to be orders of magnitude better than that of IE (Bakr and Mannseth, 79th SEG Annual Meeting, SEG Expanded Abstracts, 669-673). In the present paper, we investigate numerically the range of validity of SIE in 3D with respect to variation in problem parameters (frequency, electric conductivity, etc.). It is found that the accuracy of SIE is very good for vertically thin resistive targets for typical marine CSEM frequencies. The accuracy is also quite stable wrt. target shape and conductivity contrast, especially for resistive targets.

Introduction

For an in-line source-receiver geometry, the marine CSEM response from a thin resistive target is much more due to galvanic effects than to inductive effects (Eidesmo et al. (2002); MacGregor and Sinha (2000)). Typically, very low source frequencies (0.05 – 1 Hz) are applied.

The detection of a potential petroleum reservoir is achieved through inversion of electromagnetic data acquired in sea floor receivers. Inversion of electromagnetic data requires a number of repeated solves of the mathematical/numerical model in an iteration process. The computational efficiency of the solver will therefore have great impact of the computational efficiency of the inversion. Various types of solvers, like finite difference, finite element, integral equation (IE), and hybrid methods, have been applied. The different types of methods have different computational advantages and disadvantages. With rigorous IE (Hursán and Zhdanov (2002)), a dense-matrix problem must be solved. For problems involving many grid cells in the target region, a huge computational effort is then needed.

Recently, a novel approximate hybrid method has been shown to produce excellent accuracy in modeling the CSEM response from petroleum reservoirs in a 2D setting (Bakr and Mannseth (2009b)). This method – termed simplified IE (SIE) modeling – fully utilizes that the low-frequency CSEM response from a thin resistive body is dominated by the galvanic effect. The dense-matrix part of IE can then be replaced by sparse-matrix calculations corresponding to solving a Poisson equation for the reservoir. In Bakr and Mannseth (2009a) it was found that both theoretical and practical computational performance of SIE were orders of magnitude better than that of IE when a large number of grid cells was needed to discretize the target.

In the present paper, our main concern is to investigate the range of validity of SIE modeling in 3D with respect to variation in problem parameters such as source frequency, electric conductivity, target shape and target size. While a more extensive investigation into these issues, including also a theoretical investigation (in preparation), is beyond the scope of the extended-abstract format, we focus here on presenting some numerical results to illustrate the main features.

Integral equation approach

With rigorous IE (see, e.g., Hursán and Zhdanov (2002)), the computational effort is dominated by solving an integral equation for the anomalous electric field

$$\mathbf{E}^a(\mathbf{r}') = \int_D \mathbf{G}_E(\mathbf{r}'|\mathbf{r}) \sigma^a(\mathbf{r}) (\mathbf{E}^b(\mathbf{r}) + \mathbf{E}^a(\mathbf{r})) dV \quad (1)$$

for $\mathbf{r}' \in D$ (see, e.g., Zhdanov (2002)), leading to a dense-matrix linear system. Here, \mathbf{G}_E denotes the electric Green's tensor, σ denotes the electric conductivity, \mathbf{E} denotes the electric field, while the superscripts b and a denote background and anomalous quantities, respectively. Hence, the conductivity, σ , equals $\sigma^b + \sigma^a$ in D , while the conductivity outside D equals σ^b . For the computation of \mathbf{G}_E and \mathbf{E}^b in D , as well as the computation of \mathbf{E}^b and \mathbf{E}^a in the receivers when equation 1 has been solved, we refer to, e.g., Zhdanov (2002).

Simplified IE approach

SIE replaces the computationally intensive calculation of \mathbf{E}^a in D from equation 1 by solving

$$\nabla \cdot (\sigma \nabla U) = \nabla \cdot (\sigma^a \mathbf{E}^b), \quad (2)$$

$$\mathbf{E}^a = -\nabla U, \quad (3)$$

for \mathbf{E}^a in D , leading to a sparse-matrix linear system. When \mathbf{E}^a in D has been calculated, \mathbf{E} is found in the receivers with low computational effort, using standard equations for rigorous IE modeling. We refer to Bakr and Mannseth (2009b) for the derivation of equations 2–3, and to Bakr and Mannseth (2009a) for a description of appropriate boundary conditions for 2.

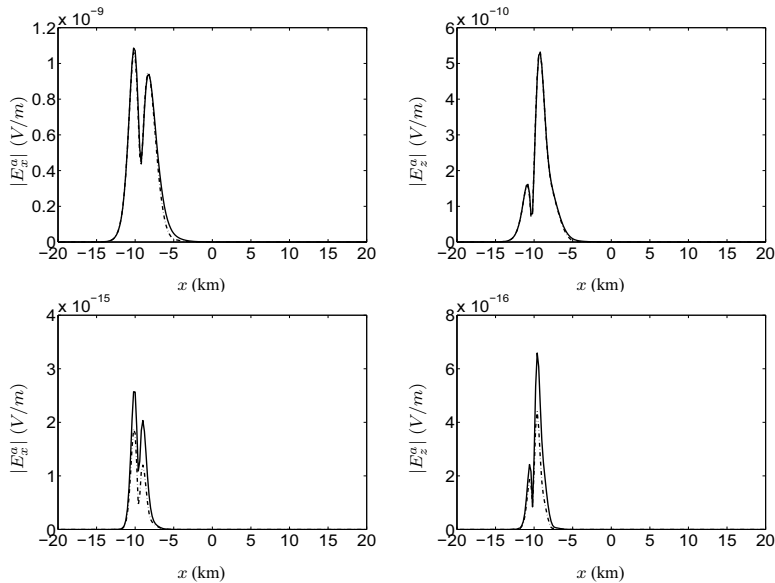


Figure 1 Simulation 1: Amplitudes $|E_x^a|$ (left panel) and $|E_z^a|$ (right panel) obtained with IE (solid line) and SIE (dash-dot line) as functions of position along the sea floor, for $f = 1$ Hz (top panel) and $f = 10$ Hz (bottom panel).

Numerical comparison

We compare computational results obtained with SIE to results obtained with rigorous IE (Hursán and Zhdanov (2002)) with respect to accuracy. (We refer to Bakr and Mannseth (2009a) for a comparison of computational cost.) Results (extracted from a more extensive numerical comparison) are shown for a test model consisting of a homogeneous half space with electric conductivity $\sigma^b = 1 \text{ S m}^{-1}$, under a 1000 m thick sea water column with electric conductivity 3.33 S m^{-1} . The source is a 100 m long, 1000 A, x -directed ($y = 0$) horizontal electric dipole, operating at frequency f , whose center location is 100 m above the sea floor and 1000 m to the left of the edge of D , along the negative x -axis. The receivers are placed in a single line along the sea floor at $y = 0$. All positions specified later will refer to a coordinate system with origin at the horizontal sea-air interface right above the centroid of the top surface of D , and where the positive z -axis points downwards. The results to be shown are amplitudes of *anomalous* electric field components in the receivers.

Simulation 1: Generic petroleum reservoir; vertically thin resistive target. The coordinates of the anomaly, D , are selected as $x \in [-10, 10]$ km, $y \in [-10, 10]$ km, $z \in [2.5, 2.55]$ km, while the electric conductivity in D is selected as $\sigma_D = 0.01 \text{ S m}^{-1}$. Figure 1, top panel, shows results for $f = 1$ Hz, while the bottom panel shows results for $f = 10$ Hz. The accuracy of SIE is quite good in this situation for frequencies smaller than about 10 Hz, and it improves when the frequency decreases. Although not illustrated here, the accuracy is stable with respect to the horizontal extension of the target, and to the conductivity contrast.

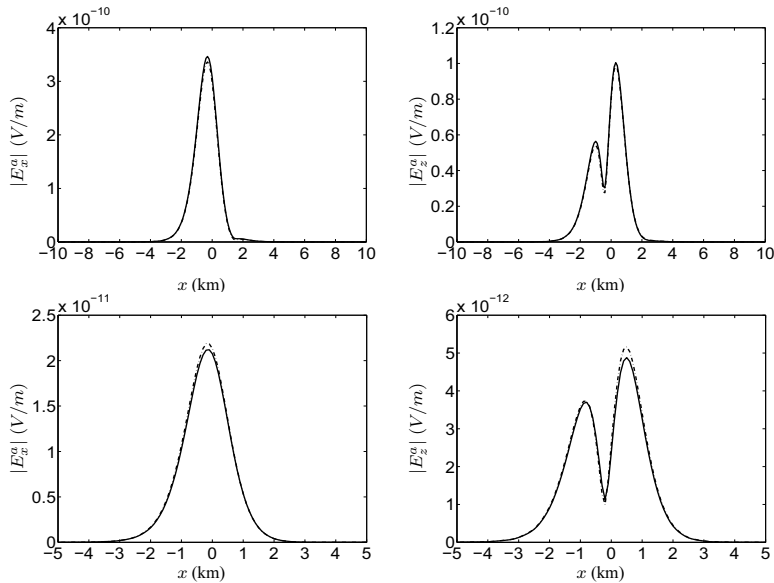


Figure 2 Simulation 2: Amplitudes $|E_x^a|$ (left panel) and $|E_z^a|$ (right panel) obtained with IE (solid line) and SIE (dash-dot line) as functions of position along the sea floor, for $f = 1$ Hz. The size of the anomaly, D , is $(500, 500, 500) \text{ m}^3$ (top panel) and $(100, 100, 1000) \text{ m}^3$ (bottom panel).

Simulation 2: Variation in target shape. It is also of interest to test the accuracy of SIE for other target shapes than that of a generic petroleum reservoir. Hence, we consider resistive targets with different shapes and volumes. The frequency and the conductivity are selected as $f = 1$ Hz and $\sigma_D = 0.01 \text{ S m}^{-1}$, respectively. Figure 2, top panel, shows results for a cubic target where D is defined by $x \in [-0.25, 0.25] \text{ km}$, $y \in [-0.25, 0.25] \text{ km}$, $z \in [-0.25, 0.25] \text{ km}$. Figure 2, bottom panel, shows results for a horizontally thin target where D is given by $x \in [-50, 50] \text{ m}$, $y \in [-50, 50] \text{ m}$, $z \in [2.5, 3.5] \text{ km}$. Comparing also with Figure 1, the accuracy of SIE modeling is seen to be stable with respect to target shapes. For a cubically shaped body, however, results (not shown here) indicate that the accuracy of SIE deteriorates somewhat as the target volume increases.

Simulation 3: Conductive target. We continue by testing SIE modeling on conductive targets with different shapes. We note that metal ores represent conductive targets, although the target shapes presented here are not selected specifically with that in mind. The frequency is selected as $f = 1$ Hz. Figure 3, top panel, shows results for a vertically thin target where D is given by $x \in [-10, 10] \text{ km}$, $y \in [-10, 10] \text{ km}$, $z \in [2.5, 2.55] \text{ km}$, while the bottom panel shows results for a horizontally thin target where D is given by $x \in [-50, 50] \text{ m}$, $y \in [-50, 50] \text{ m}$, $z \in [2.5, 3.5] \text{ km}$. The conductivity, σ_D , equals 10 S m^{-1} in the left panel and 100 S m^{-1} in the right panel. The accuracy of SIE is good also for conductive targets, but in contrast to the resistive case, it deteriorates somewhat with the strength of the conductivity contrast. Also, it is somewhat more dependent on target shape.

Conclusions

We have presented a numerical investigation to study the range of validity of SIE modeling. It was found that the accuracy is excellent for a vertically thin resistive target for typical marine CSEM frequencies,

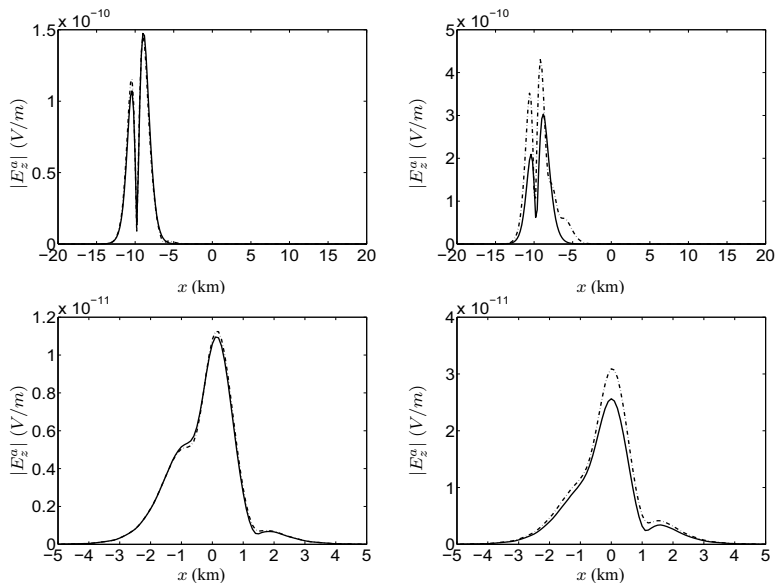


Figure 3 Simulation 3: Amplitude $|E_z^a|$ obtained with IE (solid line) and SIE (dash-dot line) as functions of position along the sea floor, for $f = 1$ Hz. The size of the anomaly, D , is $(20, 20, 0.05)$ km^3 (top panel) and $(100, 100, 1000)$ m^3 (bottom panel). The conductivity, σ_D , equals 10 S m^{-1} (left panel) and 100 S m^{-1} (right panel).

and quite good for frequencies up to about 10 Hz. For a resistive target, the accuracy of SIE was found to be very stable with respect to target shapes and volumes, and with respect to conductivity contrast strength. For a conductive target, the accuracy is also quite good, but it deteriorates somewhat with the strength of the conductivity contrast.

Acknowledgements

The first author is grateful for financial support of VISTA, a research cooperation between the Norwegian Academy of Science and Letters and StatoilHydro, to perform this study. The authors also gratefully acknowledge the Consortium for Electromagnetic Modeling and Inversion at the University of Utah for providing the IE code, INTEM3D.

References

- Bakr, S.A. and Mannseth, T. [2009a] Fast 3d modeling of the CSEM response of petroleum reservoirs. *79th Annual International Meeting, SEG, Expanded Abstracts*, 669–673.
- Bakr, S.A. and Mannseth, T. [2009b] Feasibility of simplified integral equation modeling of low-frequency marine CSEM with a resistive target. *Geophysics*, **74**(5), F107–F117.
- Eidesmo, T. et al. [2002] Sea Bed Logging (SBL), a new method for remote and direct identification of hydrocarbon filled layers in deepwater areas. *First Break*, **20**, 144–152.
- Hursán, G. and Zhdanov, M.S. [2002] Contraction integral method in three-dimensional electromagnetic modeling. *Radio Science*, **37**, 1089.
- MacGregor, L.M. and Sinha, M.C. [2000] Use of marine controlled source electromagnetic sounding for sub-basalt exploration. *Geophysical Prospecting*, **48**, 1091–1106.
- Zhdanov, M. [2002] *Geophysical inverse theory and regularization problems*. Elsevier, Amsterdam–New York–Tokyo.